Japanese Journal of Applied Physics

The Japan Society of Applied Physics

REGULAR PAPER

Low-pressure sustainment of surface-wave microwave plasma with modified microwave coupler

To cite this article: Kensuke Sasai *et al* 2016 *Jpn. J. Appl. Phys.* **55** 016203

Japanese Journal of Applied Physics 55, 016203 (2016)
http://doi.org/10.7567/JJAP.55.016203

REGULAR PAPER

Low-pressure sustainment of surface-wave microwave plasma with modified microwave coupler

Kensuke Sasai, Haruka Suzuki, and Hirotaka Toyoda

Department of Electrical Engineering and Computer Science, Nagoya University, Nagoya 464-8603, Japan

*E-mail: toyoda@nuee.nagoya-u.ac.jp

Received August 7, 2015; revised October 2, 2015; accepted October 7, 2015; published online December 9, 2015

Sustainment of long-scale surface-wave plasma (SWP) at pressures below 1 Pa is investigated for the application of the SWP as an assisting plasma source for roll-to-roll sputter deposition. A modified microwave coupler (MMC) for easier surface-wave propagation is proposed, on the basis of the concept of the power direction alignment of the slot antenna and surface-wave propagation. The superiority of the MMC-SWP over conventional SWPs is shown at a sustainment pressure as low as 0.6 Pa and an electron density as high as $3 \times 10^{17}\,m^{-3}$. A polymer film is treated with the MMC-SWP at a low pressure of 0.6 Pa, and surface modification at a low pressure is proved using Ar plasma. These results show the availability of the MMC-SWP as the surface treatment plasma source that is compatible with sputter deposition in the same processing chamber.

1. Introduction

Recently, highly functional polymer-based films for printable electronics or flexible electronics have been given attention, and development of a surface treatment process for adhesion improvement or contaminant removal has become an important issue. As a surface treatment technique, wet processing has been reported to be effective.[1] However, this technique is not suitable from an environmental viewpoint because of the consequential need for liquid waste treatment. As one of the surface treatment processes, plasma surface treatments using reduced pressures,[2–8] atmospheric pressure,[8–11] or ion beams[12–15] have been reported, but the process throughput is not sufficient for high-speed roll-to-roll sputter deposition, and an alternative high-density plasma is desired. As a candidate to solve such an issue, a surface-wave plasma (SWP) source, i.e., a microwave plasma source with no magnetic field, is attractive. So far, the plasma production mechanism of the SWP has been extensively studied,[16–20] and on the basis of these studies, its beneficial properties such as high plasma density, low ion-induce damage, and applicability to large areas[21–27] have been clarified with their deposition and etching process applications.[28–31] Furthermore, the SWP has been applied to surface modification of non-heat-resistant polymer films.[32–34] However, recent film processes require pretreatment of the film surface immediately before sputter deposition without exposure of the film surface to atmosphere. This means that the plasma source for the pre-treatment should be in the same roll-to-roll processing chamber for sputter deposition and the pre-treatment plasma source should be maintained at the same pressure as that of the sputtering process (<1 Pa). The SWP, however, is difficult to sustain at low pressures (<1 Pa). So far, many studies of microwave plasmas combined with a sputtering process have been reported,[35–38] but most of the plasma sources are used as an ECR plasma source assisted by the magnetic field of the sputter target. Some studies without using a magnetic field have been reported, but the lowest sustainable pressure is higher than sputter deposition pressures and SWPs that are maintained at low pressures, which are compatible with sputter deposition, have never been reported.

In this study, a one-dimensionally long SWP that can be sustained at low pressures (<1 Pa) is examined. For low-pressure plasma sustainment, a modified microwave coupler (MMC) is introduced into the SWP source. The properties of the MMC-SWP, such as minimum sustainment pressure or electron density, are reported in comparison with those of conventional SWPs. As an example of MMC-SWP applications, polymer surface modification is presented.

2. Modified microwave coupler for low-pressure SWP sustainment

For the sustainment of the SWP, an important point is the direction of microwave propagation. The SWP is based on the surface-wave propagation along the plasma-dielectric interface, which enables the distribution of microwave power along the dielectric–plasma interface and the production of a large-area SWP. From the viewpoint of plasma sustainment, the microwave electric field in the transverse-magnetic mode (TM-mode) SW accelerates electrons toward the plasma perpendicularly to the dielectric surface.[20] In general, the microwave power from a waveguide is usually coupled to the plasma through the slot antenna, i.e., a small rectangular narrow-gap hole opened to the waveguide. The direction of the microwave power radiation from the slot antenna is perpendicular to the slot surface; this means that the arrangement of the slot antenna and the dielectric plate is a critical issue for easier microwave coupling to the plasma. In conventional SWPs, slot antennas are arranged on the back surface of a dielectric plate, as shown in Fig. 1(a), and the microwave is radiated from the slot antennas to the direction perpendicular to the dielectric surface, i.e., perpendicular to the direction of SWP propagation. This means that, for the sustainment of the SWP, high plasma densities that deflect the microwave power direction by 90° are required, suggesting difficulty in sustaining plasma at low pressures.

To improve the microwave coupling and low-pressure sustainment, we modified the slot-dielectric configuration; the slot antenna is placed on the side wall of the dielectric plate, as shown in Fig. 1(b). Hereafter, we call this configuration as the MMC. In the case of the MMC-SWP, the power radiation from the slot is parallel to the dielectric surface and a much easier sustainment of the surface-wave is expected.

To verify this concept, a numerical simulation is carried out using the electromagnetic wave simulation software MW-Studio. Schematics of the simulation models of the conven-

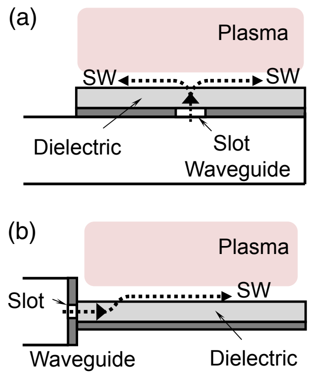

Fig. 1. (Color online) Schematic of microwave power coupling configurations for (a) conventional SWP and (b) SWP with modified microwave coupler.

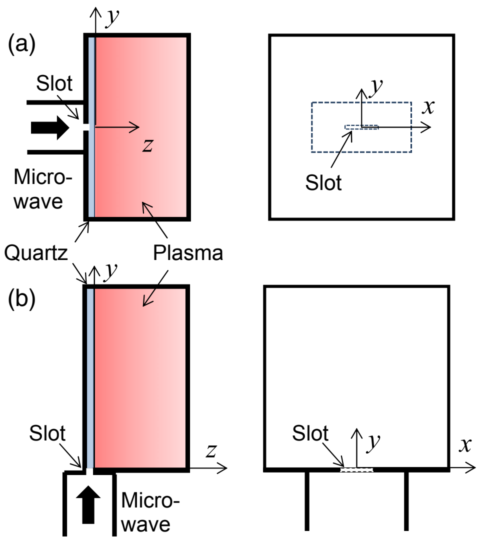

Fig. 2. (Color online) Modeled structure for the numerical simulation. (a) Conventional SWP and (b) MMC-SWP.

tional SWP and MMC-SWP are shown in Figs. 2(a) and 2(b), respectively. In this simulation, one rectangular slot antenna with the same size as that shown in the figure ($35 \times 5\,\mathrm{mm}^2$, 2 mm in thickness) is set at the end of a waveguide ($109.2 \times 54.6\,\mathrm{mm}^2$ in cross section). Supposing a quartz plate, a $20 \times 20\,\mathrm{cm}^2$ dielectric plate with a thickness of 1 cm and a relative permittivity (ε_r) of 3.7 is attached to the slot antenna at two different configurations, i.e., from the back side of the dielectric (conventional SWP) and from the sidewall of the dielectric (MMC-SWP). Then, a plasma space ($20 \times 20 \times 10\,\mathrm{cm}^3$) with electron densities from 2 to $6 \times 10^{17}\,\mathrm{m}^{-3}$ and a collision frequency of 4.0×10^7 Hz is placed adjacent to the dielectric plate. A wave packet of 2.45 GHz microwave is injected into the waveguide, and the response of the electromagnetic wave inside the modeled space is calculated using a finite integration (FI) simulation method. After the Fourier transform of the time-domain simulated result, 2.45 GHz continuous wave (CW) propagation in the modeled space is obtained.

Figure 3 shows a contour map of electric field amplitude at the dielectric–plasma interface at an electron density of $3.8 \times 10^{17}\,\mathrm{m}^{-3}$, which is slightly higher than the surface-wave resonance density ($3.5 \times 10^{17}\,\mathrm{m}^{-3}$ for $f = 2.45$ GHz and

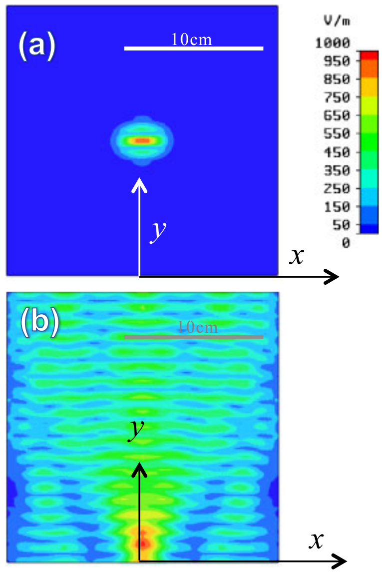

Fig. 3. (Color online) Spatial profile of simulated microwave electric field at the position of plasma–quartz interface. (a) Conventional SWP and (b) SWP with modified microwave coupler. The electron density is $3.8 \times 10^{17}\,\mathrm{m}^{-3}$.

$\varepsilon_r = 3.7$). The input power into the waveguide is supposed to be a unit value of 1 W. The electric field at an arbitrary input power can be obtained considering that the electric field is proportional to the square root of the input power. In both cases of conventional SWP and MMC-SWP, the maximum electric fields are almost the same (~1 kV/m at an input power of 1 W). From the viewpoint of wave propagation, however, the electric field is quite different depending on the slot configuration. In the case of conventional SWP, the electric field is localized in the vicinity of the slot. In the case of MMC-SWP, wave propagation along the interface in the y-direction is clearly observed.

It has been reported that the SWP is sustained by the high-energy electrons injected into the plasma perpendicular to the dielectric surface. Such high-energy electrons are produced by a strong electric field in the vicinity of the plasma boundary where the permittivity of the plasma is close to zero, i.e., the plasma oscillation frequency is 2.45 GHz. This means that the microwave electric field perpendicular to the dielectric surface plays an important role in the sustainment of the SWP. On the basis of this plasma sustainment mechanism, the component of the perpendicular microwave electric field with respect to the absolute electric field is investigated in both case of conventional SWP and MMC-SWP. Figure 4 shows the ratio of the squared perpendicular electric field component (E^2_{perp}) to the total field energy ($|E|^2$) as a function of electron density. Here, both E^2_{perp} and $|E|^2$ are obtained as average values along the y-axis. In both cases of conventional and modified SWPs, the perpendicular field energy component monotonically decreases with decreasing electron density. In the case of conventional SWPs, the perpendicular field energy component decreases almost down to zero at an electron density of $4 \times 10^{17}\,\mathrm{m}^{-3}$. In the case of MMC-SWP, however, the perpendicular component remains even below the surface-wave resonant density of $3.5 \times 10^{17}\,\mathrm{m}^{-3}$, suggesting the sustainment of the hybrid-mode SWP.[39] The simulation result suggests that the position of the slot with respect

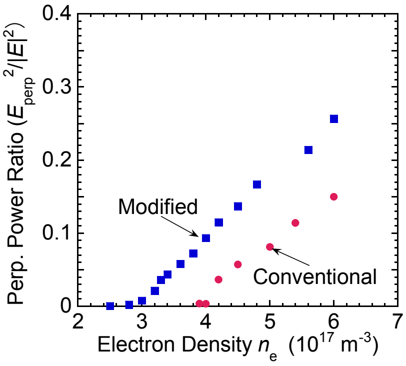

Fig. 4. (Color online) Ratio of perpendicular electric field component to absolute electric field component averaged along y-axis as a function of electron density. (a) Conventional SWP and (b) SWP with modified microwave coupler.

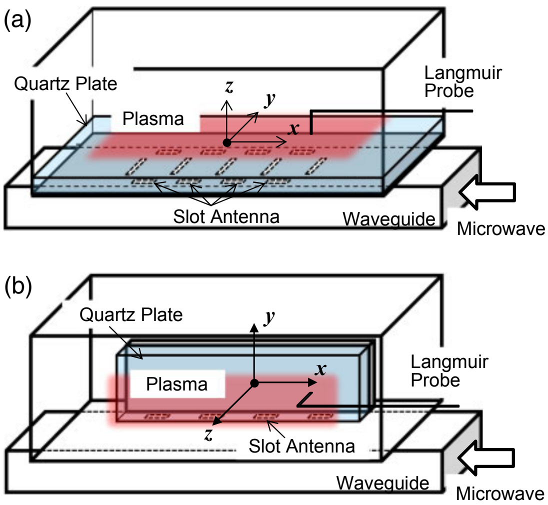

Fig. 5. (Color online) Schematic of experimental set up for (a) conventional SWP and (b) SWP with modified microwave coupler.

to the dielectric plate has a very important role in the sustainment of an SWP and that the plasma can be sustained at lower pressures using the MMC-SWP.

3. Experimental methods

To confirm the validity of the MMC-SWP concept, the lowest sustainable pressures are compared between conventional and MMC-SWPs. In the experiment, an aluminum chamber (length, 1.2 m; width, 0.7 m; height, 0.6 m) is evacuated using a turbomolecular pump at base pressures below 10^{-3} Pa. Ar gas is introduced into the chamber through a mass flow controller and the pressure is controlled at values below 13 Pa. Two types of SWP source, i.e., conventional SWP and MMC-SWP, are compared, as shown in Fig. 3. In the experiment of conventional SWP [Fig. 5(a)], the microwave power (2.45 GHz, <1.6 kW) from 13 slots is coupled to the plasma through a quartz dielectric plate (length, 368 mm; width, 145 mm; thickness, 15 mm) that is adjacent to the slot plate. The dielectric plate works as a vacuum window and also as the dielectric material that enables surface-wave propagation along the dielectric surface. The origin of the coordinates is set to be the surface of the quartz center, and the x-, y-, and z-axes are defined as shown in the figure.

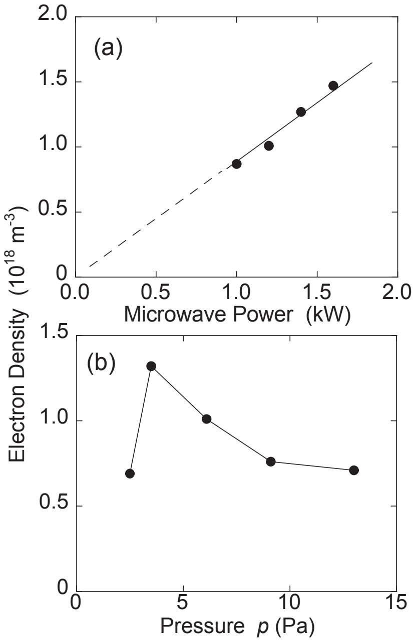

Fig. 6. Langmuir probe measurement of electron density for conventional SWP. (a) Power dependence and (b) pressure dependence.

The configuration of the modified microwave coupler is shown in Fig. 5(b). In this SWP source, microwave radiation is realized by four vacuum-sealed slot antennas that are attached to the side wall of a quartz plate (length, 400 mm; width, 60 mm; thickness, 20 mm). In this configuration, microwave power propagates along the quartz plate smoothly and the plasma is produced in front of the quartz plate surface. This plasma source is installed in a chamber similar to that shown Fig. 5(a). The spatial profile of electron density is measured by scanning a Langmuir probe (length, 5 mm; diameter, 0.2 mm) at a bias voltage of 50 V. Electron density is obtained from the saturation current supposing that the same electron temperature is obtained at the center of the target ($x = 0$). To confirm the performance of the new SWP source, films of terpolymers of tetrafluoroethylene, hexafluoropropylene, and vinylidene fluoride (THV) are treated with the MMC-SWP and their surfaces before and after the plasma treatment are analyzed by X-ray photoelectron spectroscopy (XPS).

4. Results and discussion

Figure 6(a) shows the electron density of the conventional SWP source as a function of microwave power at an Ar pressure of 6 Pa and a position of $x = 0$ cm, $y = 0$ cm, and $z = 10$ cm. By reducing the microwave power, the electron density monotonically decreases to 0.9×10^{18} m^{-3} at a microwave power of 1.0 kW and plasma disappears at powers lower than 1 kW. Figure 6(b) shows electron density as a function of Ar pressure at a microwave power of 1.2 kW. The electron density is measured at $x = 0$ cm, $y = 0$ cm, and $z = 10$ cm. Except for the lowest Ar pressure of 2.5 Pa, the electron density monotonically increases with Ar pressure decreasing to 3.5 Pa. Such dependence is qualitatively understood as follows. As mentioned in Sect. 2, a strong microwave electric field of the SW accelerates electrons perpendicularly to the dielectric surface and these high-energy

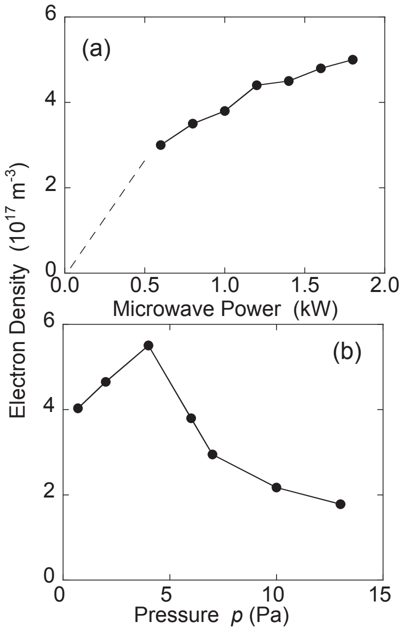

Fig. 7. Langmuir probe measurement of electron density for MMC-SWP. (a) Power dependence and (b) pressure dependence.

electrons pass through the plasma along the z-direction. The kinetic energy of high-energy electrons decreases as the electrons pass through the gas phase owing to their collisions with Ar, resulting in the decreases in ionization efficiency and electron density along the z-axis. With increasing Ar pressure, the electron-energy decay length decreases and plasma becomes localized in the vicinity of the dielectric surface, resulting in the decrease in electron density at higher pressures. The result indicating that the electron density at a pressure of 2.5 Pa is lower than that at 3.5 Pa implies the difficulty in plasma sustainment at pressures lower than 3.5 Pa with the conventional SWP source.

Next, a similar measurement is carried out with the MMC-SWP. Figure 7(a) shows electron density as a function of microwave power in the case of MMC-SWP. Measurement conditions are the same as those shown in Fig. 6(a), i.e., the probe position is $x = 0$ cm, $y = 0$ cm, and $z = 10$ cm and the Ar pressure is 6 Pa. As in the case of conventional SWP, the electron density is almost proportional to the microwave power, and an electron density of 5×10^{17} m^{-3} is obtained at a microwave power of 1.8 kW. It is notable that the plasma is sustained even at a microwave power of 0.6 kW, at which the plasma cannot be sustained by a conventional SWP. This suggests the ease of producing the MMC-SWP, i.e., better coupling of microwave power to the plasma. Figure 7(b) shows the Ar pressure dependence of electron density at a microwave power of 1.0 kW. The probe position is $x = 0$ cm, $y = 0$ cm, and $z = 10$ cm. As in the case of conventional SWP, the electron density monotonically increases with decreasing the Ar pressure and shows a peak. The peak plasma density is obtained at an Ar pressure of 4 Pa, which is similar to that of the conventional SWP. It is notable that plasma is sustained at an Ar pressure of 0.7 Pa with an electron density of 5×10^{17} m^{-3}, although the microwave power is lower than that of the conventional SWP [Fig. 6(b)]. The result shows the superior property of the MMC-SWP for low-pressure plasma sustainment. Figure 8 shows a spatial

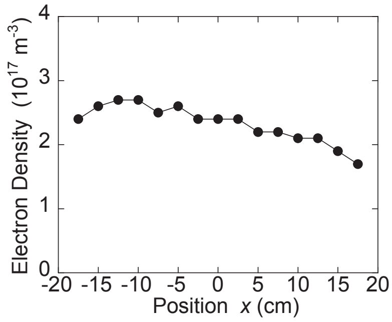

Fig. 8. Spatial profile of electron density for MMC-SWP.

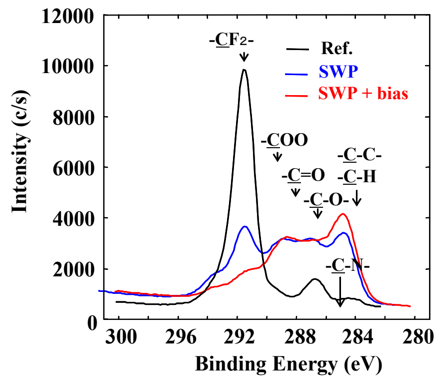

Fig. 9. (Color online) C 1s XPS spectra of THV film before and after Ar plasma treatment with and without RF bias.

profile of electron density along the x-axis at a microwave power of 1.0 kW and an Ar pressure of 6 Pa. The probe position is $y = 0$ cm and $z = 15$ cm. Although a slight variation of electron density is observed along the x-axis, the density deviation between $z = \pm 15$ cm is $\pm 12\%$ at a mean electron density of 2.3×10^{17} m^{-3}. With decreasing pressure, the uniformity of the emission along the x-axis is almost the same, although a slight decrease in the emission intensity along the y-axis from the slot is observed. When considering the use of MMC-SWP for roll-to-roll film process, the plasma source requires a uniform electron density more than a wide range of film widths. The result suggests the applicability of the MMC-SWP for the pre-treatment of the roll-to-roll sputter deposition system using the same processing chamber.

Finally, the polymer film is treated with the MMC-SWP and the treatment performance is investigated. In the experiment, a THV film sample is set 10 cm away from the quartz plate ($x = y = 0$, $z = 10$ cm) on a stage of 10×30 cm^2. The Ar pressure and microwave power are 0.6 Pa and 1.2 kW, respectively. Figure 9 shows the XPS spectra of C 1s before and after the Ar plasma treatment using the MMC-SWP. The result for the film sample treated at an RF bias power of 0.6 kW is also shown in Fig. 9. Samples are treated using the MMC-SWP for 30 s, exposed to the atmosphere for transport, and measured using the XPS system. Before the plasma treatment, a strong peak originating from the CF_2 bond is observed at a binding energy of 292 eV. After the plasma treatment, however, the CF_2 peak is suppressed and, instead, increases in COOH, C–O, CN, and C=O peaks at 284–290 eV are observed. Application of RF bias power further decreases the CF_2 peak with a slight increase in the intensity of the CN bond. The increase in O- or N-related peaks after the plasma treatment indicates that the plasma-activated surface produces these bonds during sample exposure to the atmosphere.

5. Conclusions

For the development of a roll-to-roll processing system that includes both plasma treatment and sputter deposition in the same processing chamber, a high-density SWP source that sustains plasma at low pressures below 1 Pa was investigated. The MMC for easier surface-wave propagation was proposed, on the basis of the concept of the power direction alignment of the slot antenna and surface-wave propagation. The superiority of the MMC-SWP over conventional SWPs for low-pressure plasma sustainment was investigated by numerical simulations and experiments. The MMC-SWP source showed Ar plasma sustainment even at a pressure of 0.7 Pa with high electron density ($5 \times 10^{17}\,m^{-3}$). A polymer film (THV) was treated with the MMC-SWP at a low pressure of 0.6 Pa, and surface modification at a low pressure was proved using Ar plasma. These results show the applicability of the MMC-SWP as the surface treatment plasma source that is compatible with sputter deposition in the same processing chamber.

Acknowledgement

Part of this work was supported by Japan Science and Technology (JST) Program of R&D for Innovative Research.

1) S.-M. Ho, T.-H. Wang, H.-L. Chen, K.-M. Chen, S.-M. Lian, and A. Hung, J. Appl. Polym. Sci. **51**, 1373 (1994).
2) N. Inagaki, S. Tasaka, and K. Hibi, J. Polym. Sci. **30**, 1425 (1992).
3) N. Inagaki, S. Tasaka, and M. Masumoto, Macromolecules **29**, 1642 (1996).
4) S. H. Kim, S. W. Na, N.-E. Lee, Y. W. Nam, and Y.-H. Kim, Surf. Coatings Technol. **200**, 2072 (2005).
5) C.-H. Yang, S.-C. Lee, J.-M. Wu, and T.-C. Lin, Appl. Surf. Sci. **252**, 1818 (2005).
6) D. Bhusari, H. Hayden, R. Tanikella, S. A. B. Allen, and P. A. Kohl, J. Electrochem. Soc. **152**, F162 (2005).
7) K. Katoh, T. Motobe, M. Ohe, K. Soejima, Y. Kaneya, T. Tanaka, and T. Itabashi, J. Photopolym. Sci. Technol. **22**, 393 (2009).
8) J. S. Eom and S. H. Kim, Thin Solid Films **516**, 4530 (2008).
9) S. H. Kim, S. H. Cho, N.-E. Lee, H. M. Kim, Y. W. Nam, and Y.-H. Kim, Surf. Coatings Technol. **193**, 101 (2005).
10) S. B. Lee and Y.-K. Kim, Plasma Processes Polym. **6**, S525 (2009).
11) J. Borris, A. Dohse, A. Hinze, M. Thomas, C.-P. Klages, A. Mobius, D. Elbick, and E.-R. Weidlich, Plasma Processes Polym. **6**, S258 (2009).
12) G. S. Chang, S. M. Jung, Y. S. Lee, I. S. Choi, C. N. Whang, J. J. Woo, and Y. P. Lee, J. Appl. Phys. **81**, 135 (1997).
13) A. M. Ektessabi and S. Hakamata, Thin Solid Films **377–378**, 621 (2000).
14) W. J. Lee and Y. B. Kim, Thin Solid Films **517**, 1191 (2008).
15) D.-H. Park and W.-K. Choi, Thin Solid Films **517**, 4222 (2009).
16) M. M. Glaude, M. Moisan, R. Pentel, P. Leprince, and J. Marec, J. Appl. Phys. **51**, 5693 (1980).
17) M. Moisan, A. Shivarova, and A. W. Trivelpiece, Plasma Phys. **24**, 1331 (1982).
18) E. Mateev, I. Zhelyazkov, and V. Atanassov, J. Appl. Phys. **54**, 3049 (1983).
19) M. Moisan and Z. Zakrzewski, in *Microwave Excited Plasmas*, ed. M. Moisan and J. Pelletier (Elsevier, Amsterdam, 1992) p. 123.
20) C. M. Ferreira and M. Moisan, in *Surface Waves in Plasmas and Solids*, ed. S. Vukovic (World Scientific, Singapore, 1985) p. 113.
21) M. Moisan, C. M. Ferreira, J. Hubert, J. Margot, and Z. Zakrzewski, in *Phenomena in Ionized Gases*, ed. K. H. Becker and W. E. Carr (AIP Press, New York, 1995) p. 25.
22) T. Ishijima, H. Toyoda, Y. Takanishi, and H. Sugai, Jpn. J. Appl. Phys. **50**, 036002 (2011).
23) I. Ghanashev, M. Nagatsu, and H. Sugai, Jpn. J. Appl. Phys. **36**, 337 (1997).
24) M. Nagatsu, G. Xu, I. Ghanashev, M. Kanoh, and H. Sugai, Plasma Sources Sci. Technol. **6**, 427 (1997).
25) I. Ghanashev, M. Nagatsu, G. Xu, and H. Sugai, Jpn. J. Appl. Phys. **36**, 4704 (1997).
26) H. Sugai, T. H. Ahn, I. Ghanashev, M. Goto, M. Nagatsu, K. Nakamura, K. Suzuki, and H. Toyoda, Plasma Phys. Control. Fusion **39**, A445 (1997).
27) T. Ishijima, Y. Nojiri, H. Toyoda, and H. Sugai, Jpn. J. Appl. Phys. **49**, 086002 (2010).
28) S. Somiya, H. Toyoda, Y. Hotta, and H. Sugai, Jpn. J. Appl. Phys. **43**, 7696 (2004).
29) Y. Hotta, H. Toyoda, and H. Sugai, Thin Solid Films **515**, 4983 (2007).
30) Y. Takanishi, T. Okayasu, H. Toyoda, and H. Sugai, Thin Solid Films **516**, 3554 (2008).
31) H. Kokura, S. Yoneda, K. Nakamura, N. Mitsuhira, M. Nakamura, and H. Sugai, Jpn. J. Appl. Phys. **38**, 5256 (1999).
32) K. Ishikawa, T. Ishijima, K. Sasai, H. Toyoda, and H. Sugai, Trans. Mater. Res. Soc. Jpn. **33**, 683 (2008).
33) Y. Takagi, Y. Gunjo, H. Toyoda, and H. Sugai, Vacuum **83**, 501 (2008).
34) K. Usami, T. Ishijima, and H. Toyoda, Thin Solid Films **521**, 22 (2012).
35) C. Boisse-Laporte, O. Leroy, L. de Poucques, B. Agius, J. Bretagne, M. C. Hugon, L. Teulé-Gay, and M. Touzeau, Surf. Coatings Technol. **179**, 176 (2004).
36) F. Thièry, Y. Pauleau, and L. Ortega, J. Vac. Sci. Technol. A **22**, 30 (2004).
37) J. Musil, M. Mišina, and D. Hovorka, J. Vac. Sci. Technol. A **15**, 1999 (1997).
38) L. de Poucques, J. C. Imbert, P. Vasina, C. Boisse-Laporte, L. Teulé-Gay, J. Bretagne, and M. Touzeau, Surf. Coatings Technol. **200**, 800 (2005).
39) I. Ghanashev, M. Nagatsu, S. Morita, and H. Sugai, J. Vac. Sci. Technol. A **16**, 1537 (1998).